

SI appendix

Title: Enhancement of hepatic autophagy increases ureagenesis and protects against hyperammonemia.

Authors: Leandro R. Soria^a, Gabriella Allegri^b, Dominique Melck^c, Nunzia Pastore^{d,e}, Patrizia Annunziata^a, Debora Paris^c, Elena Polishchuk^a, Edoardo Nusco^a, Beat Thöny^b, Andrea Motta^c, Johannes Häberle^b, Andrea Ballabio^{a,d,e,f}, and Nicola Brunetti-Pierri^{a,f}

Institutions: ^aTelethon Institute of Genetics and Medicine, 80078 Pozzuoli, Italy;

^bDivision of Metabolism, University Children's Hospital Zurich and Children's Research Center, 8032 Zurich, Switzerland; ^cInstitute of Biomolecular Chemistry, National

Research Council, 80078 Pozzuoli, Italy; ^dDepartment of Molecular and Human Genetics; Baylor College of Medicine; 77030 Houston, TX, USA; ^eJan and Dan Duncan

Neurological Research Institute; Texas Children's Hospital; 77030 Houston, TX, USA;

^fDepartment of Translational Medicine, Federico II University, 80131 Naples, Italy.

SI appendix, SI Figures

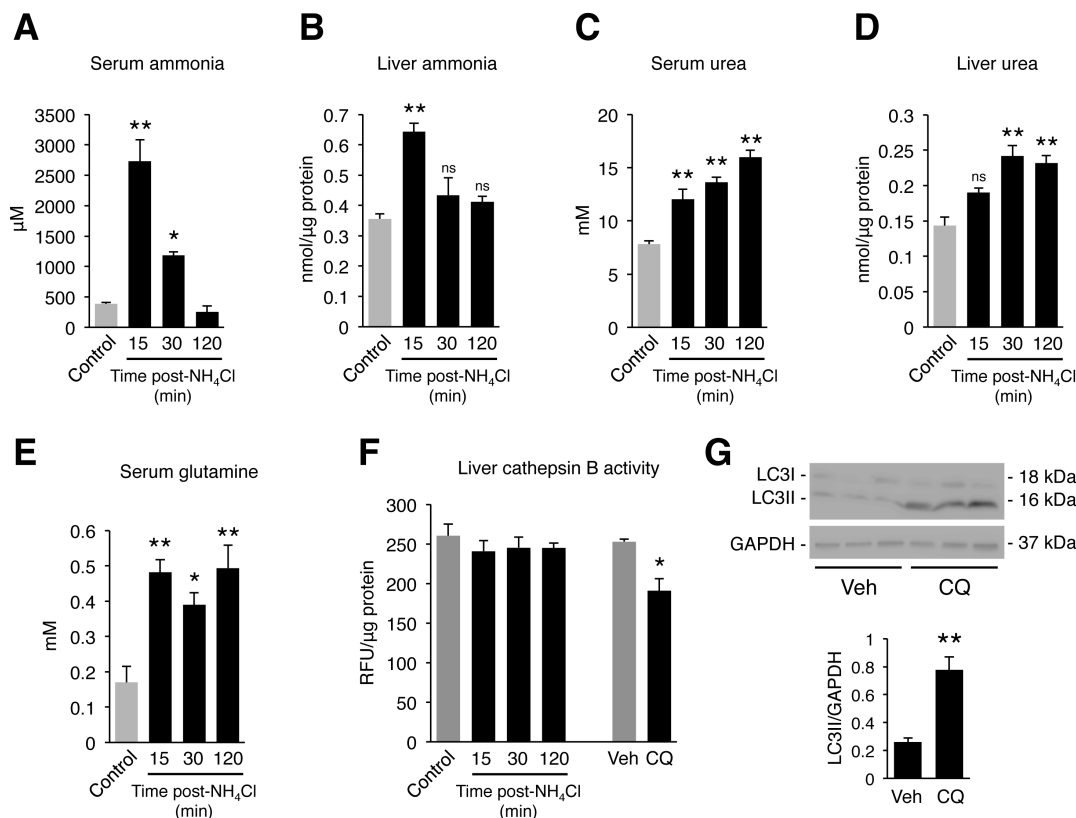


Fig. S1. Acute challenge with ammonium chloride in mice. (A-D) Serum and hepatic levels of ammonia and urea at baseline (control), 15, 30, and 120 minutes after intraperitoneal (i.p.) injections of ammonium chloride (10 mmol/kg) in wild-type (WT) C57BL/6 mice. ANOVA, Tukey's post-hoc test: $p=2.30E-06$ for **A**; $p=0.0004$ for **B**; $p=6.85E-06$ for **C**; and $p=0.0002$ for **D** ($n \geq 4$ per group). (E) Serum glutamine at baseline (control), 15, 30, and 120 minutes after i.p. injections of ammonium chloride in WT mice. ANOVA, Tukey's post-hoc test: $p=0.0013$ ($n=4$ per group). (F) Cathepsin B activity in liver lysates was unchanged after acute i.p. challenge with ammonium chloride compared to vehicle-injected controls. In contrast, positive controls of liver lysates from chloroquine-treated mice (CQ, 120 mg/kg, i.p. for 1 hour, $n=3$) showed significantly decreased cathepsin B activity and increased LC3II (**G**) compared to mice treated with vehicle (Veh, $n=3$). Unpaired Student's *t* test compared with control condition. GAPDH was used as loading control. All the values are shown as averages \pm S.E.M. * $p < 0.05$, ** $p < 0.01$. min: minutes; ns: not significant.

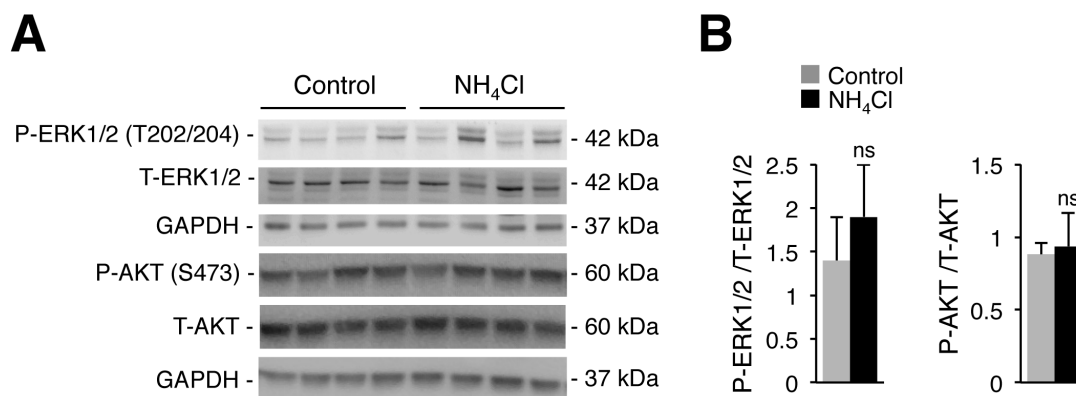


Fig. S2. Phosphorylation of kinases regulating autophagy in livers of mice with hyperammonemia. (A) Western blot analyses and densitometric quantifications (B) for P-ERK1/2, T-ERK1/2, P-AKT, and T-AKT in livers from saline- (control) and ammonia-treated WT C57BL/6 mice at 0.5 hours Pi. GAPDH was used as loading control. Data represent averages \pm S.E.M. ($n \geq 4$ per group). Pi: post-injection. ns: not significant.

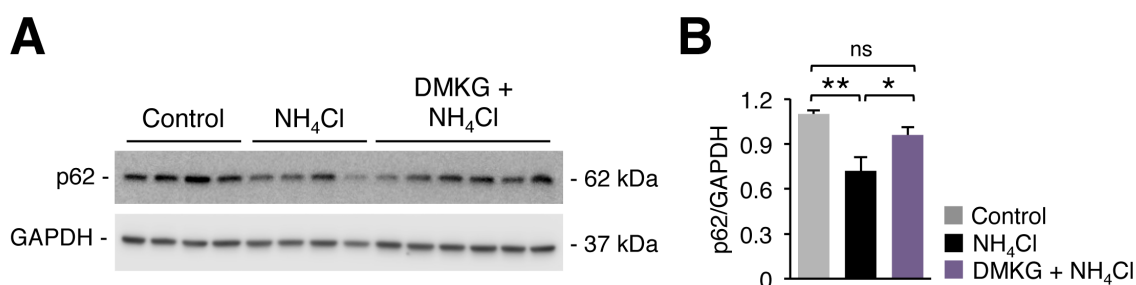


Fig. S3. Dimethyl- α -ketoglutarate prevents ammonia-induced p62 consumption. (A) Western blotting for p62 of livers harvested 0.5 hours after the injections of saline (control) or ammonium chloride (NH₄Cl) in WT C57BL/6 mice treated with Dimethyl- α -ketoglutarate (DMKG) (500 mg/kg i.p. for 3 days and 1 hour prior to the ammonia i.p. injections) or vehicle. GAPDH was used as loading control. (B) Densitometric quantifications of p62 Western blotting bands normalized to GAPDH. Averages \pm S.E.M. are shown. (Control $n=4$, NH₄Cl $n=4$, DMKG + NH₄Cl $n=6$), * $p < 0.05$, ** $p < 0.01$. ANOVA, $p = 0.0057$; Tukey's post-hoc test.

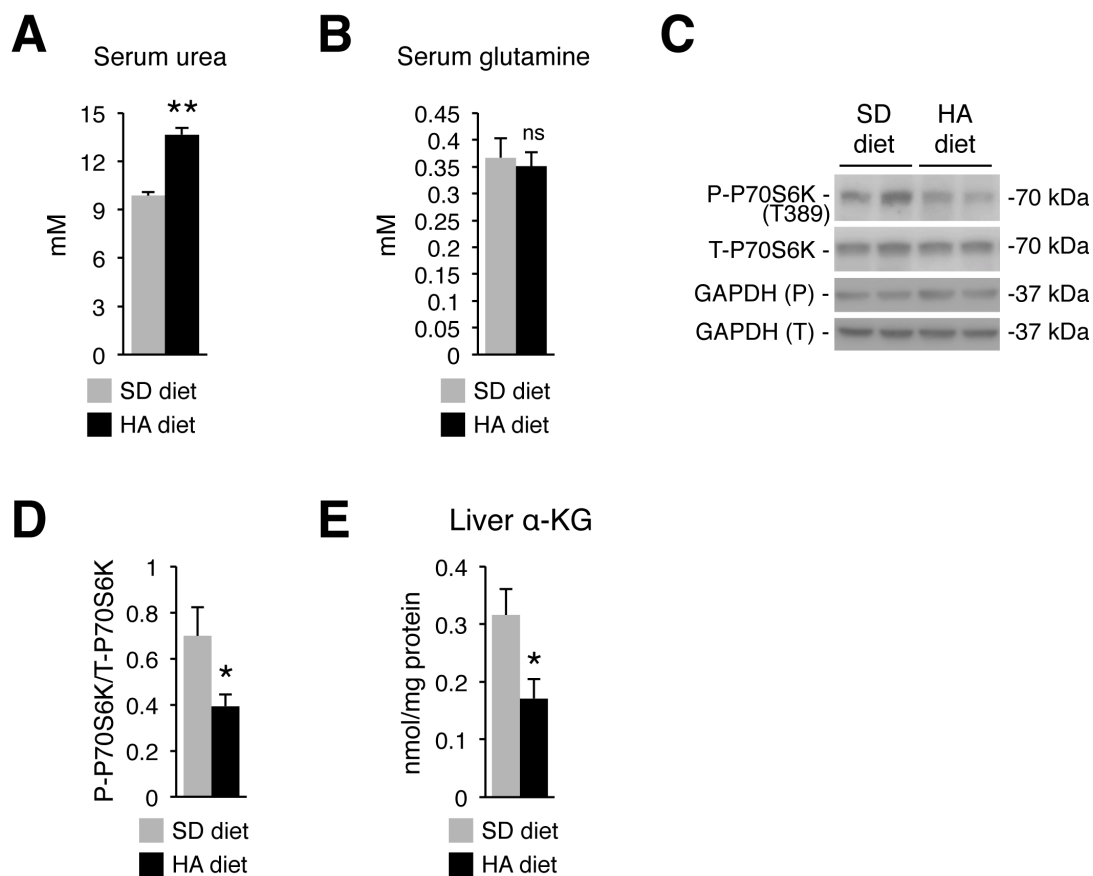


Fig. S4. Autophagy in chronic hyperammonemia. (A-B) Serum levels of urea and glutamine in WT C57BL/6 mice fed for 14 weeks with a diet containing ammonium acetate (HA diet) or with a standard diet (SD diet). Averages \pm S.E.M. are shown. $**p < 0.01$ (unpaired Student's t test) ($n \geq 6$ per group). (C-D) Western blot and densitometric quantifications of P-P70S6K and T-P70S6K in livers of mice fed for 14 weeks with a diet containing ammonium acetate (HA diet) or with a standard diet (SD diet). Averages \pm S.E.M. are shown. $*p < 0.05$ (unpaired Student's t test) ($n = 4$ per group). (E) α -ketoglutarate (α -KG) in livers of mice fed for 14 weeks with a diet containing ammonium acetate (HA diet, $n = 5$) or with a standard diet (SD diet, $n = 3$). Data represent averages \pm S.E.M. $*p < 0.05$, (unpaired Student's t test) compared with control condition. ns: not significant.

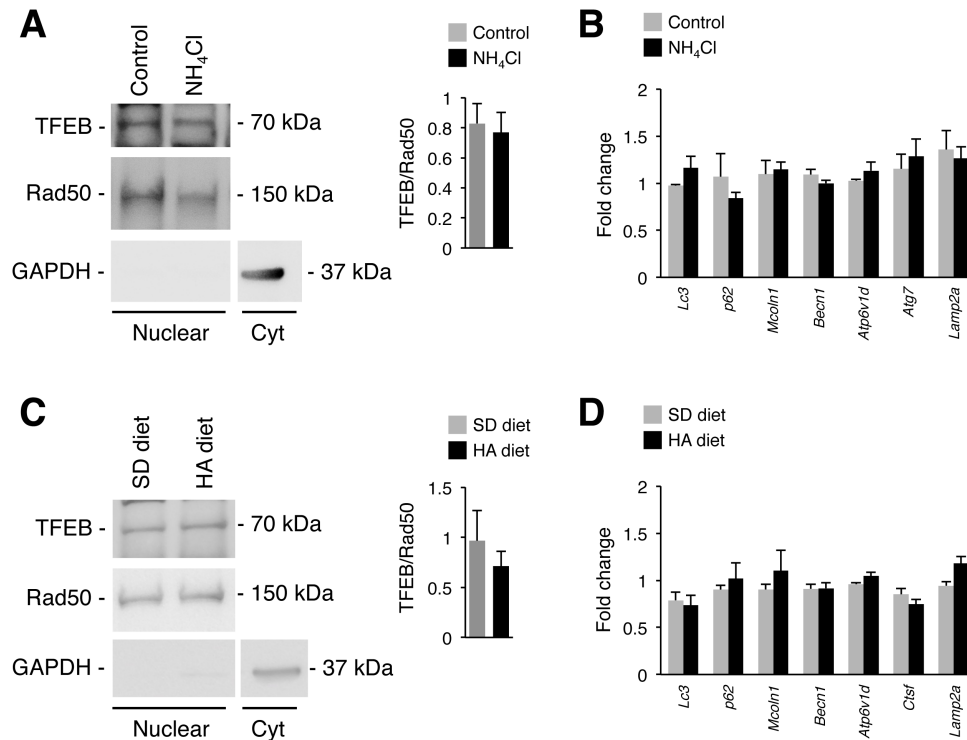


Fig. S5. TFEB nuclear translocation during acute and chronic hyperammonemia.

Western blot and densitometric quantification of TFEB in enriched nuclear cellular fractions from livers of WT C57BL/6 mice (A) harvested 30 minutes after i.p. injections of ammonium chloride (NH₄Cl) or vehicle, and (C) fed for 14 weeks with a diet containing ammonium acetate (HA diet) or a standard diet (SD diet) (n≥3 per group). Densitometric quantifications of TFEB bands were normalized to Rad50. Blots were probed with an anti-GAPDH antibody to rule out cytoplasmic contamination. Real time PCR analysis of autophagic and lysosomal genes in liver samples isolated from WT C57BL/6 mice under acute (i.p. injection) (n=3) (B), and chronic (diet-induced) (n=5) (D) hyperammonemia. Data represent averages ± S.E.M.

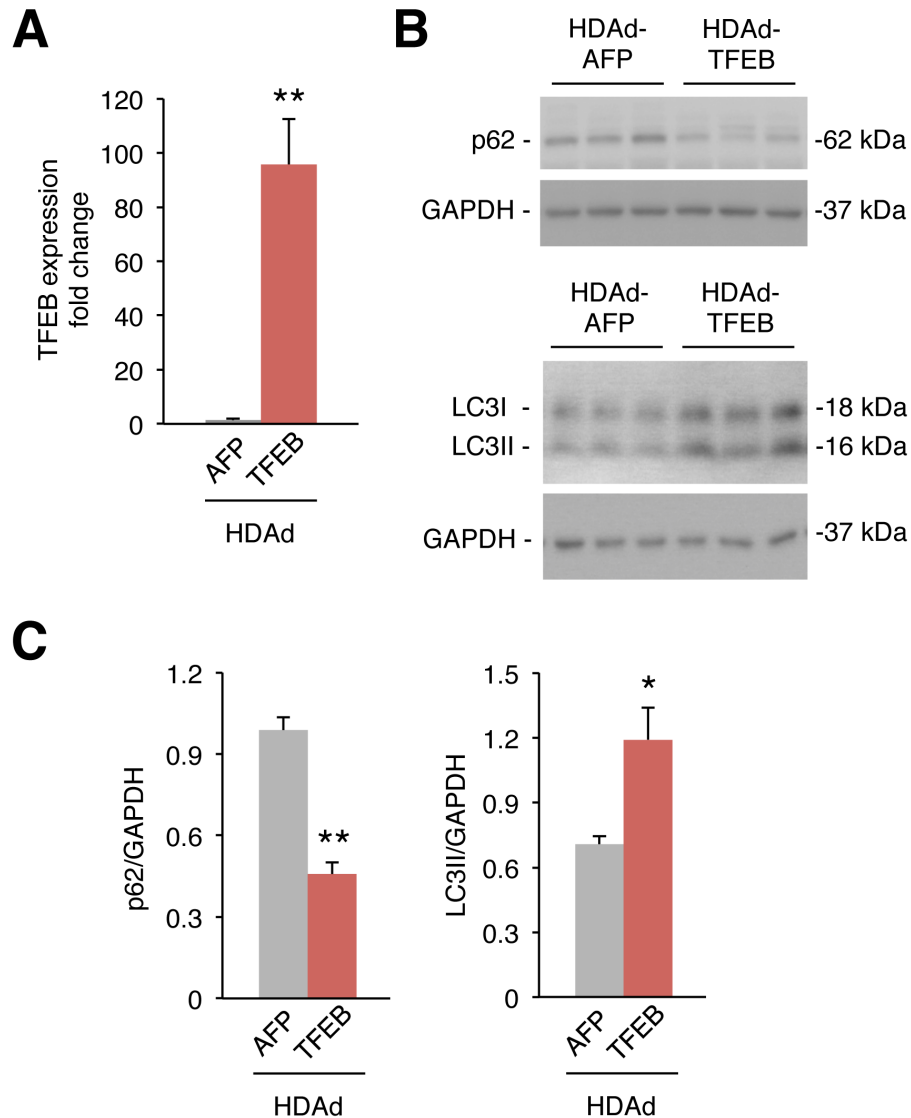


Fig. S6. Liver-directed gene transfer of human TFEB increases hepatic autophagy.

(A) TFEB real time PCR on mRNA extracted from livers 4 weeks after the injections of HDAd-TFEB or HDAd-AFP (control vector expressing unrelated transgene). $**p < 0.01$ (unpaired Student's t test) compared with control group (n=5 per group). (B) Representative Western blotting bands of p62 and LC3 in livers harvested 2.0 hours post-ammonia injection in WT C57BL/6 mice injected four weeks before with HDAd-TFEB or HDAd-AFP. GAPDH was used as loading control. (C) Densitometric quantifications. Averages \pm S.E.M. are shown. $*p < 0.05$, $**p < 0.01$ (unpaired Student's t test) compared with control group (n=5 per group).

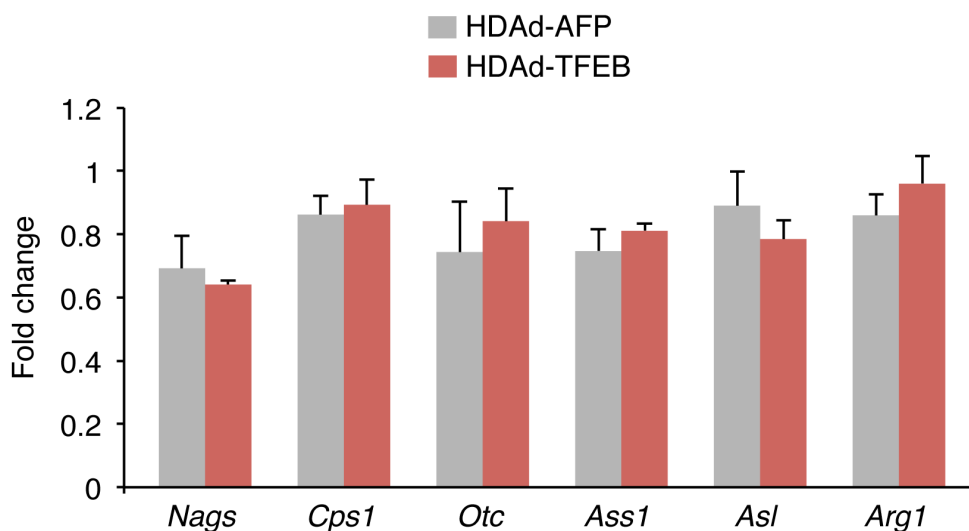


Fig. S7. Expression of urea cycle genes in HDAd-TFEB and HDAd-AFP injected mice. By real time PCR expression of genes encoding the urea cycle enzymes *Nags*, *Cps1*, *Otc*, *Ass1*, *Asl* and *Arg1* was unchanged in livers of HDAd-TFEB injected WT C57BL/6 mice compared to controls injected with HDAd-AFP at four weeks post-vector injection. Averages \pm S.E.M. are shown (n=5 per group).

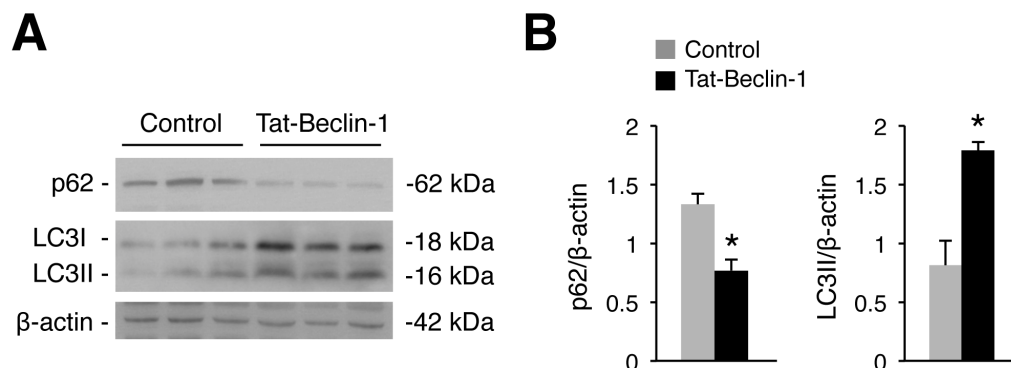


Fig. S8. Tat-Beclin-1 increases hepatic autophagy. (A) Western blotting for p62 and LC3 in livers of WT C57BL/6 mice injected with vehicle (control) or Tat-Beclin-1 (20 mg/kg i.p. 2 hours prior to sacrifice); β -actin was used as loading control. (B) Densitometric quantifications Averages \pm S.E.M. are shown. * $p < 0.05$ (unpaired Student's t test) compared with control group (n=3 per group).

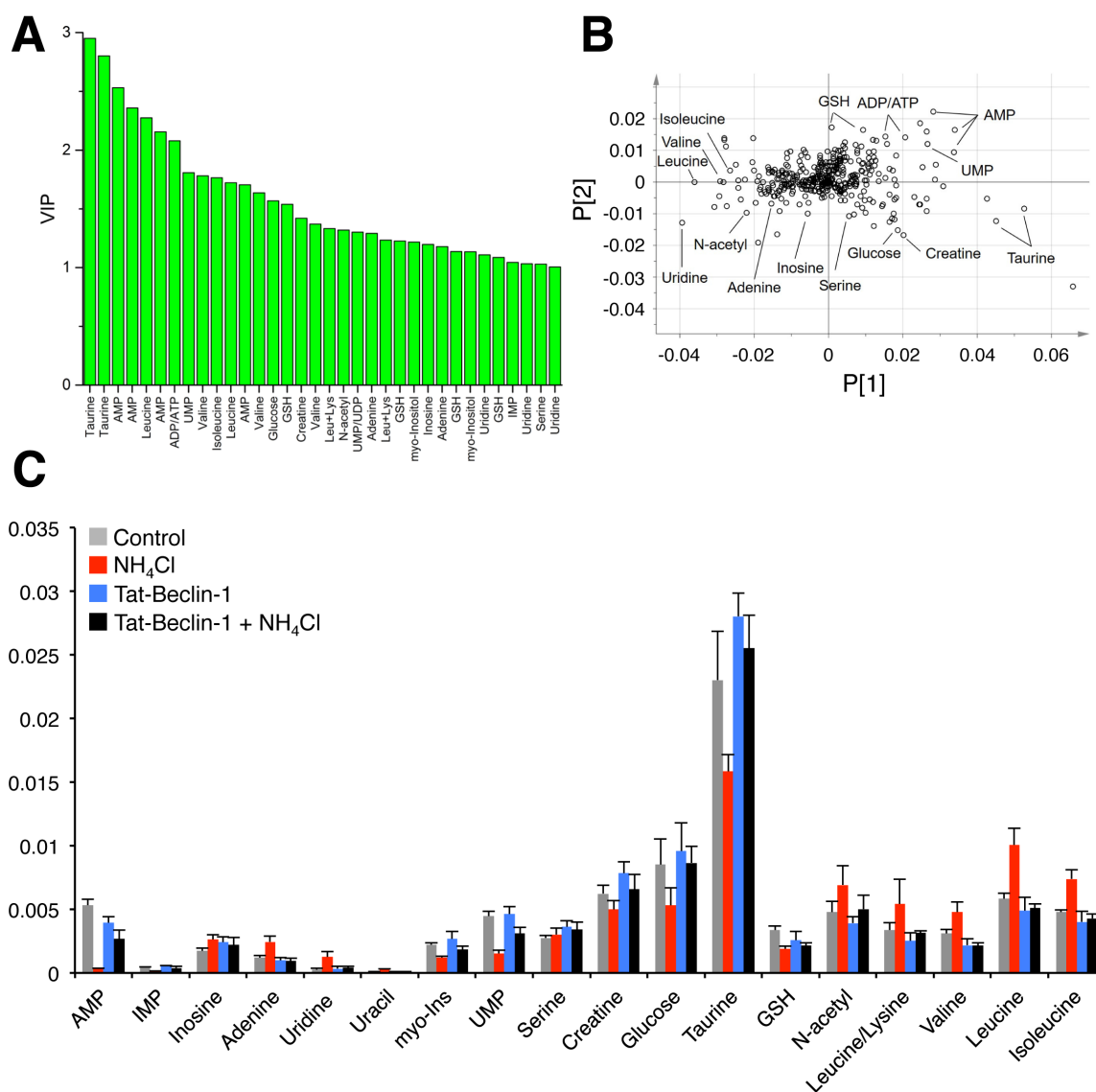


Fig. S9. Liver metabolome extended data. (A) Variable importance of projection (VIP) score plot, and loading plot (B) of the Orthogonal Projection to Latent Structure-Discriminant Analysis (OPLS-DA) model showed in **Fig. 5C**. Metabolites with high VIP values ($VIP > 1$, and $pcorr > 0.7$) are showed. (C) Liver metabolites by ¹H-NMR analysis with statistically significant differences between control WT C57BL/6 mice (grey bars) compared to mice with acute hyperammonemia (red bars) or Tat-Beclin-1 treated mice with acute hyperammonemia (black bars). Tat-Beclin-1 treated mice without hyperammonemia (blue bars) are also shown. The values are shown as averages \pm S.E.M. ($n=5$ per group).

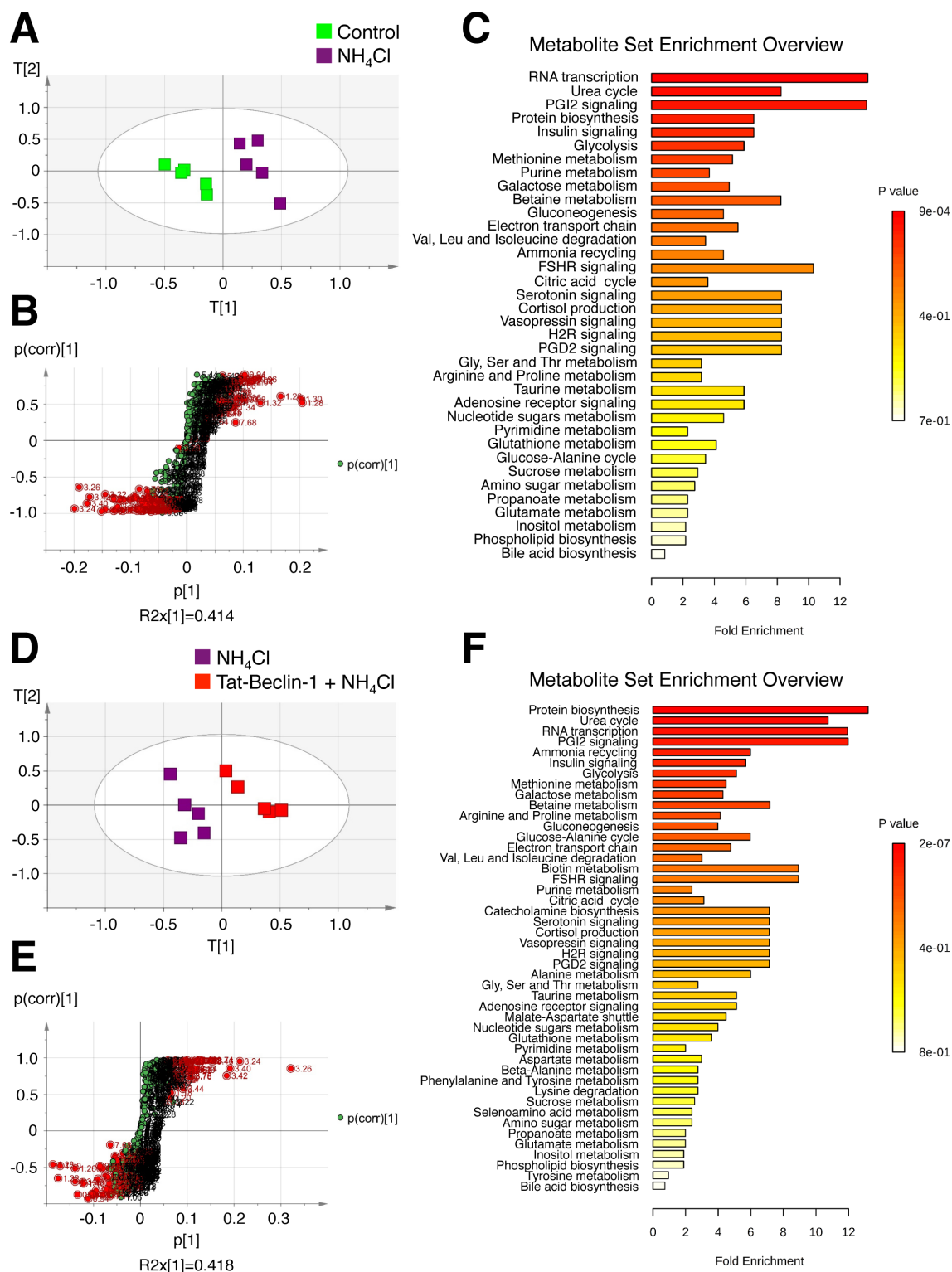


Fig. S10. Metabolic pathway analysis of metabolites dysregulated in acute hyperammonemia and restored by Tat-Beclin-1. (A) Projection to Latent Structure-Discriminant Analysis (PLS-DA) score plot showing the degree of separation between

liver extracts analysed by high resolution $^1\text{H-NMR}$ spectroscopy from control mice (green) and mice with acute hyperammonemia (violet), and **(B)** the associated S-plot identifying the variables (red dots) mostly involved in the discrimination. A robust statistical model, with parameters $R^2= 0.95$ and $Q^2=0.88$, CV-ANOVA test p value= 0.02 and 800 hits permutation test $R_{\text{fit}}= 0.40$ and $Q_{\text{fit}}=-0.39$ was obtained ($n=5$). **(C)** Metabolite set enrichment overview obtained by “Metabolite Set Enrichment Analysis” (MSEA). **(D)** Projection to Latent Structure-Discriminant Analysis (PLS-DA) score plot and S-plot **(E)** shows the degree of separation between liver extracts analysed by high resolution $^1\text{H-NMR}$ spectroscopy from mice with acute hyperammonemia (violet) and mice with acute hyperammonemia treated with Tat-Beclin-1 (red), and the most relevant variables (red dots) altered by Tat-Beclin-1 treatment. A robust statistical model, with parameters $R^2= 0.92$ and $Q^2=0.81$, CV-ANOVA test p value= 0.03 and 800 hits permutation test $R_{\text{fit}}= 0.41$ and $Q_{\text{fit}}=-0.35$ was obtained ($n=5$). **(F)** Metabolite set enrichment overview obtained MSEA showing the metabolic changes induced by the Tat-Beclin-1 treatment during hyperammonemia. For both analyses metabolites responsible for the separation between groups were selected using a combination of VIP (Variable Influence in Projection) value >1 and correlation loading values $p(\text{corr}) > 0.7$ in the PLS-DA model classification.

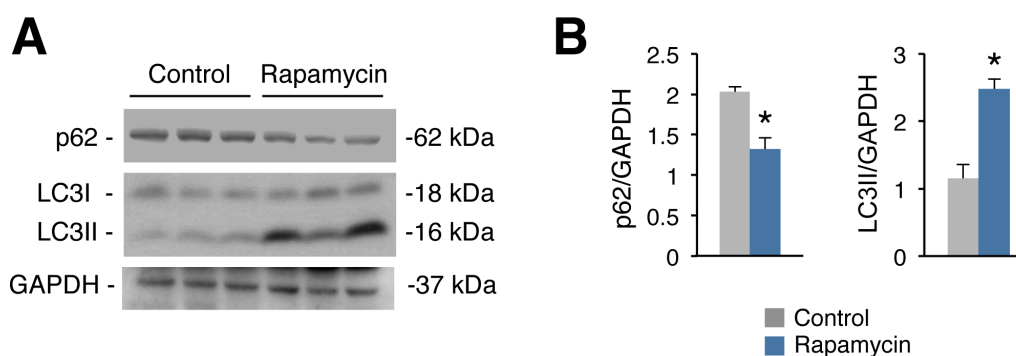


Fig. S11. Rapamycin increases autophagy in livers. **(A)** Western blotting for LC3 and p62 in livers of WT C57BL/6 mice treated with vehicle (control) or rapamycin (2 mg/kg i.p. for 3 days) harvested at 2.0 hours post-ammonia load. GAPDH was used as loading control. **(B)** Densitometric quantifications. Averages \pm S.E.M. are shown. $*p < 0.05$ (unpaired Student's t test) compared with control group ($n=3$ per group).

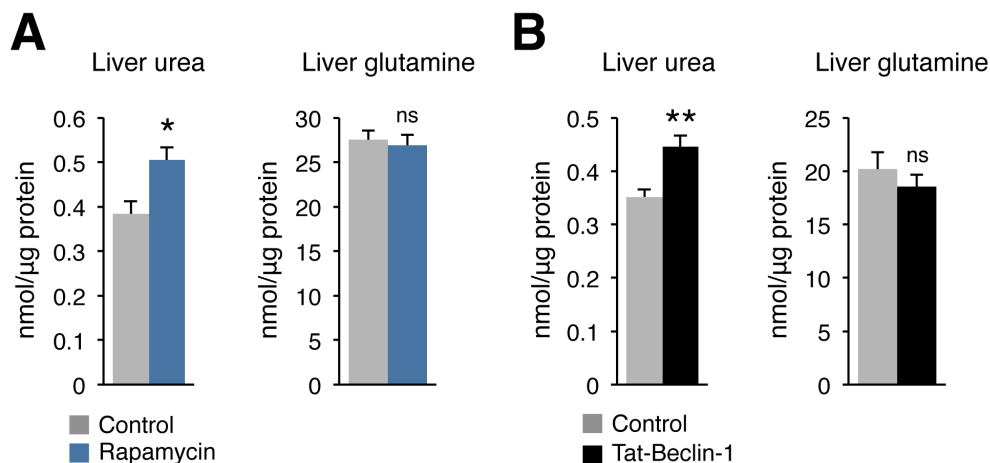


Fig. S12. Hepatic urea and glutamine in mice treated with autophagy activators. (A) Urea and glutamine in livers harvested at 2.0 hours post NH_4Cl injection in WT C57BL/6 mice injected with rapamycin (2 mg/kg i.p. for 3 days) or vehicle (n=5 for urea, and n=5 for glutamine). **(B)** Urea and glutamine in livers harvested at 1.0 hour post NH_4Cl injection in WT mice injected with Tat-Beclin-1 (20 mg/kg i.p. 2 hours prior ammonia load) or vehicle (n \geq 9 for urea, and n=5 for glutamine). All values are shown as averages \pm S.E.M. * p < 0.05, ** p < 0.01 (unpaired Student's t test). ns: not significant.

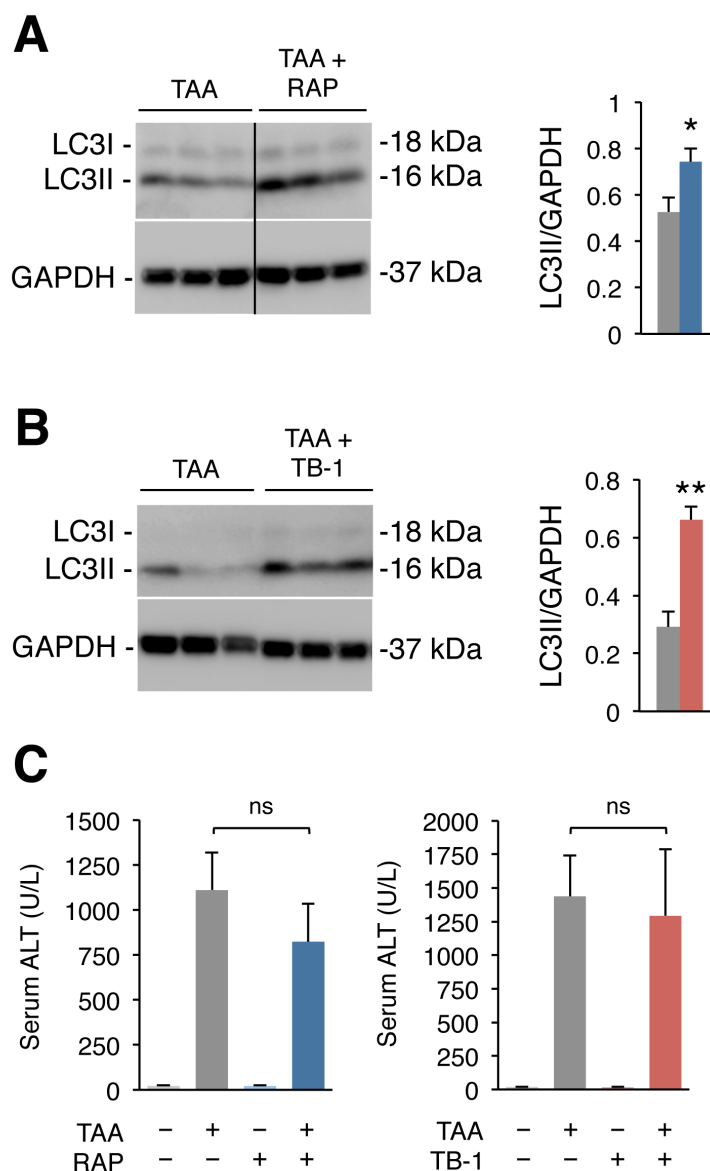


Fig. S13. Activation of liver autophagy during thioacetamide-induced liver failure. (A, B) Autophagy induction was measured by Western blot for LC3 in livers of WT C57BL/6 mice treated with the rapamycin (RAP) or Tat-Beclin-1 (TB-1) (2 mg/kg and 15 mg/kg for 3 days i.p., respectively) during the thioacetamide-induced liver failure. GAPDH was used as loading control. In A: Samples were run on the same gel but were non-contiguous (Fig. S15). (C) Serum alanine transaminase (ALT) levels, a positive control marker for liver damage. TAA: thioacetamide; ns: not significant. All values are shown as averages \pm S.E.M. * $p < 0.05$; ** $p < 0.01$; (unpaired Student's t test) compared with control group ($n \geq 5$ per group).

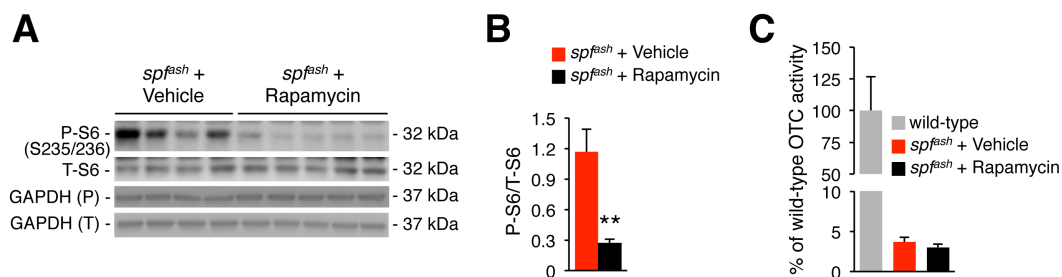


Fig. S14. Rapamycin treatment in *spf^{ash}* mice. (A, B) Western blot analyses of P-S6 and T-S6 in livers of *spf^{ash}* mice treated with rapamycin (10 mg/kg for 7 days i.p., n=5) or vehicle (n=4). GAPDH was used as loading control. (C) Liver ornithine transcarbamylase (OTC) activity in *spf^{ash}* mice injected with rapamycin or vehicle (n=4-5 per group) compared to WT levels (n=2). All values are shown as averages \pm S.E.M.; ** p < 0.01; (unpaired Student's t test) compared with the vehicle-treated group.

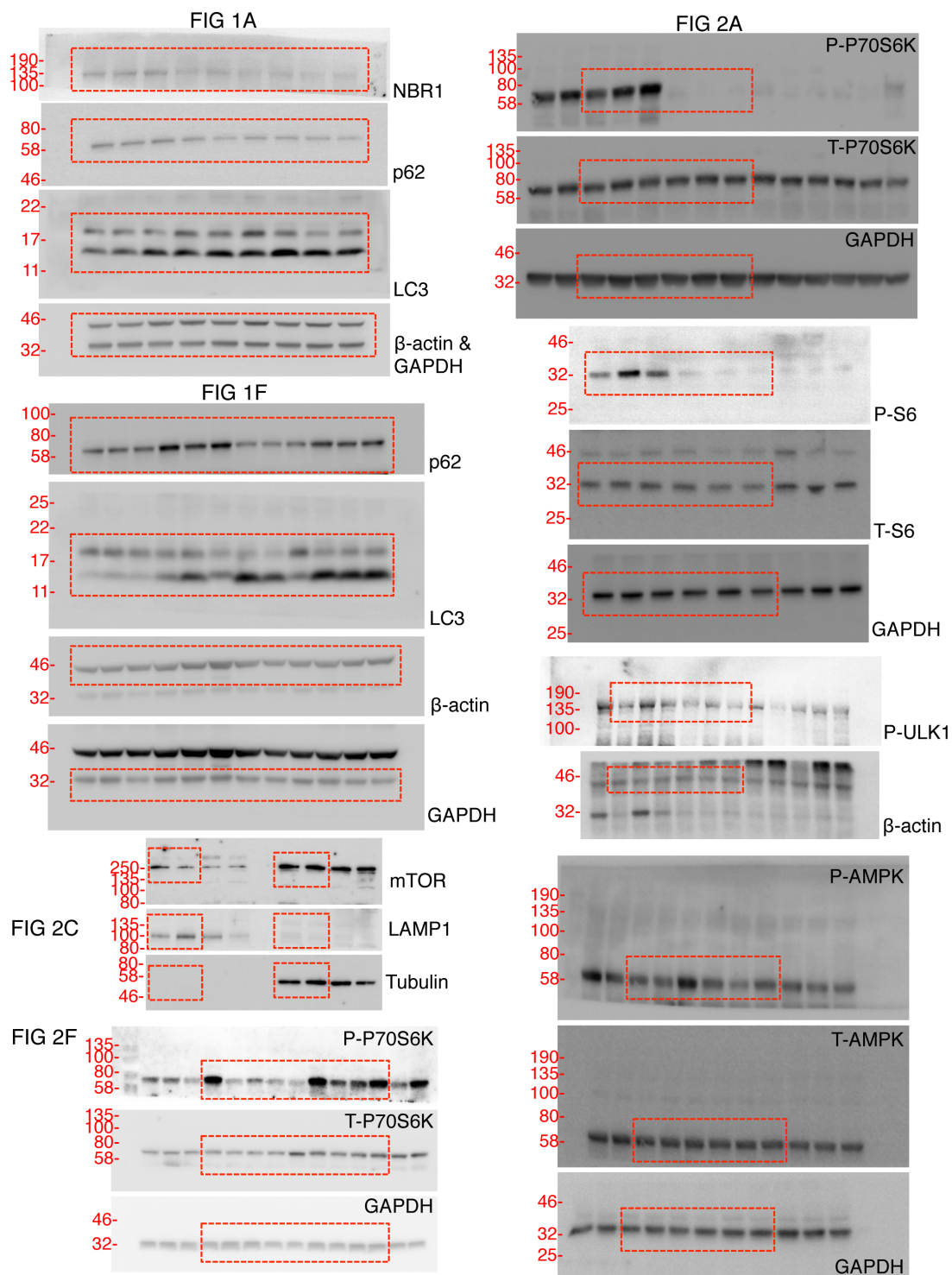


Fig. S15. Uncropped scans of western blots. Part 1.

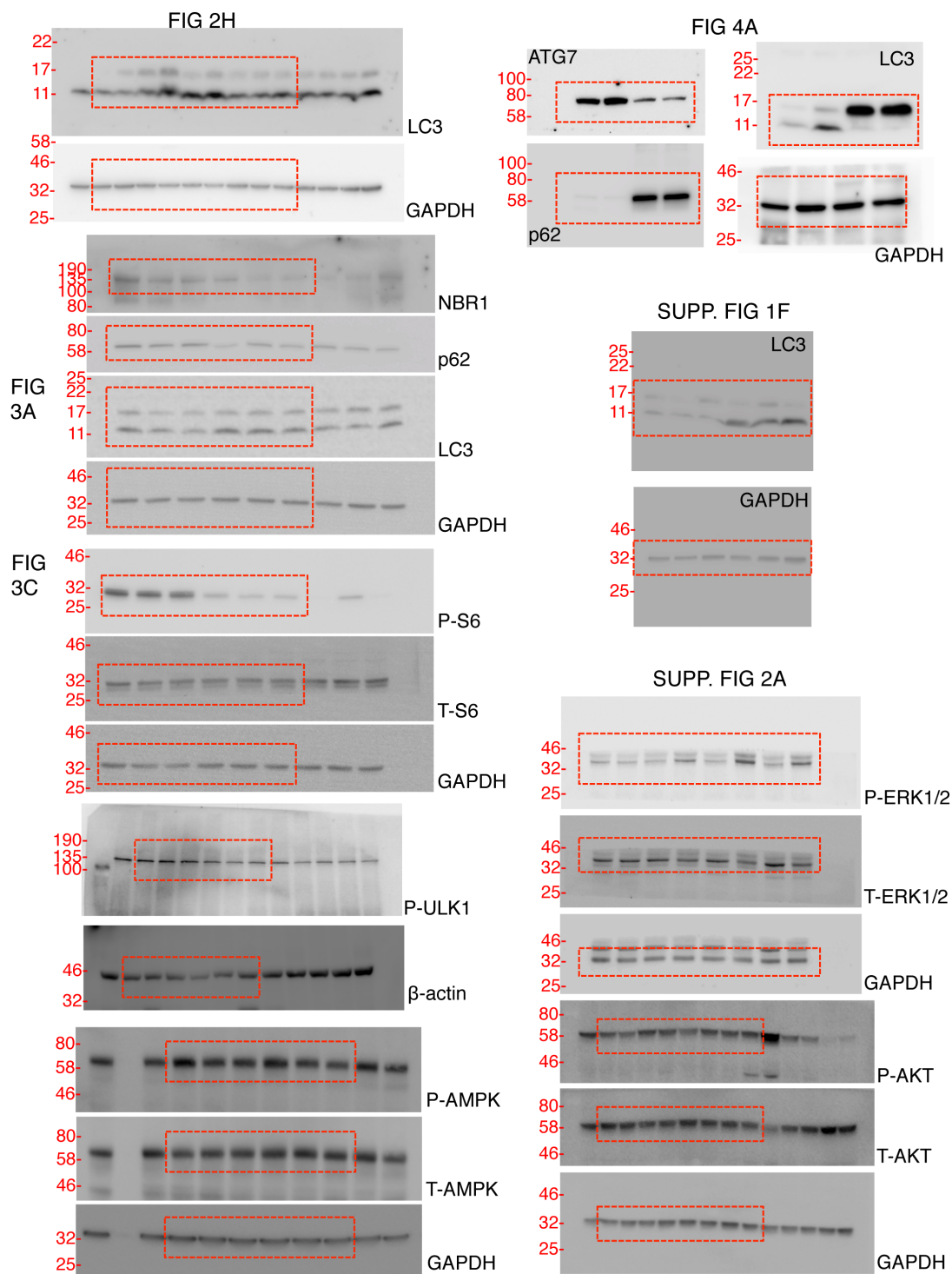


Fig. S15. Uncropped scans of western blots. Part 2.

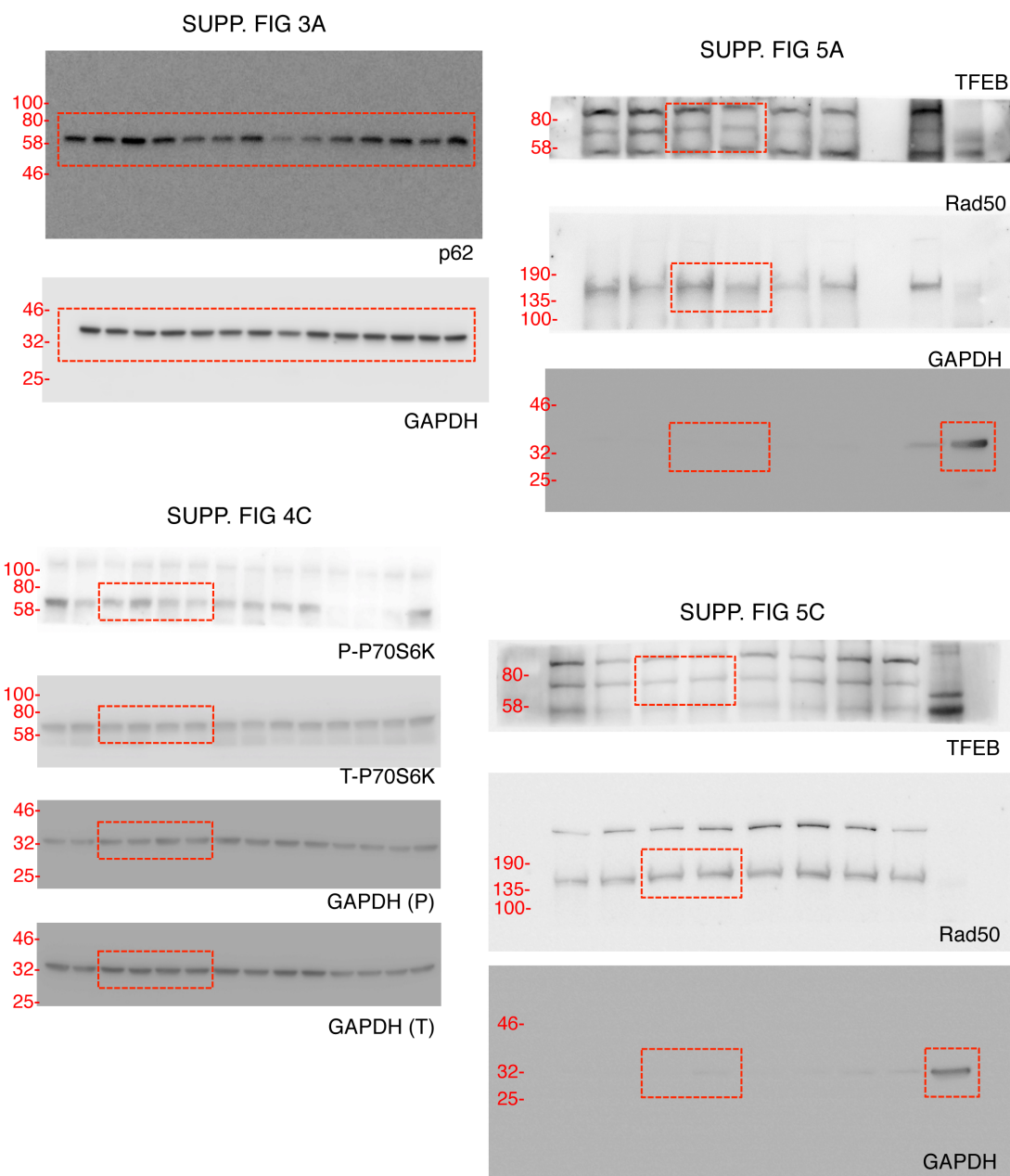


Fig. S15. Uncropped scans of western blots. Part 3.

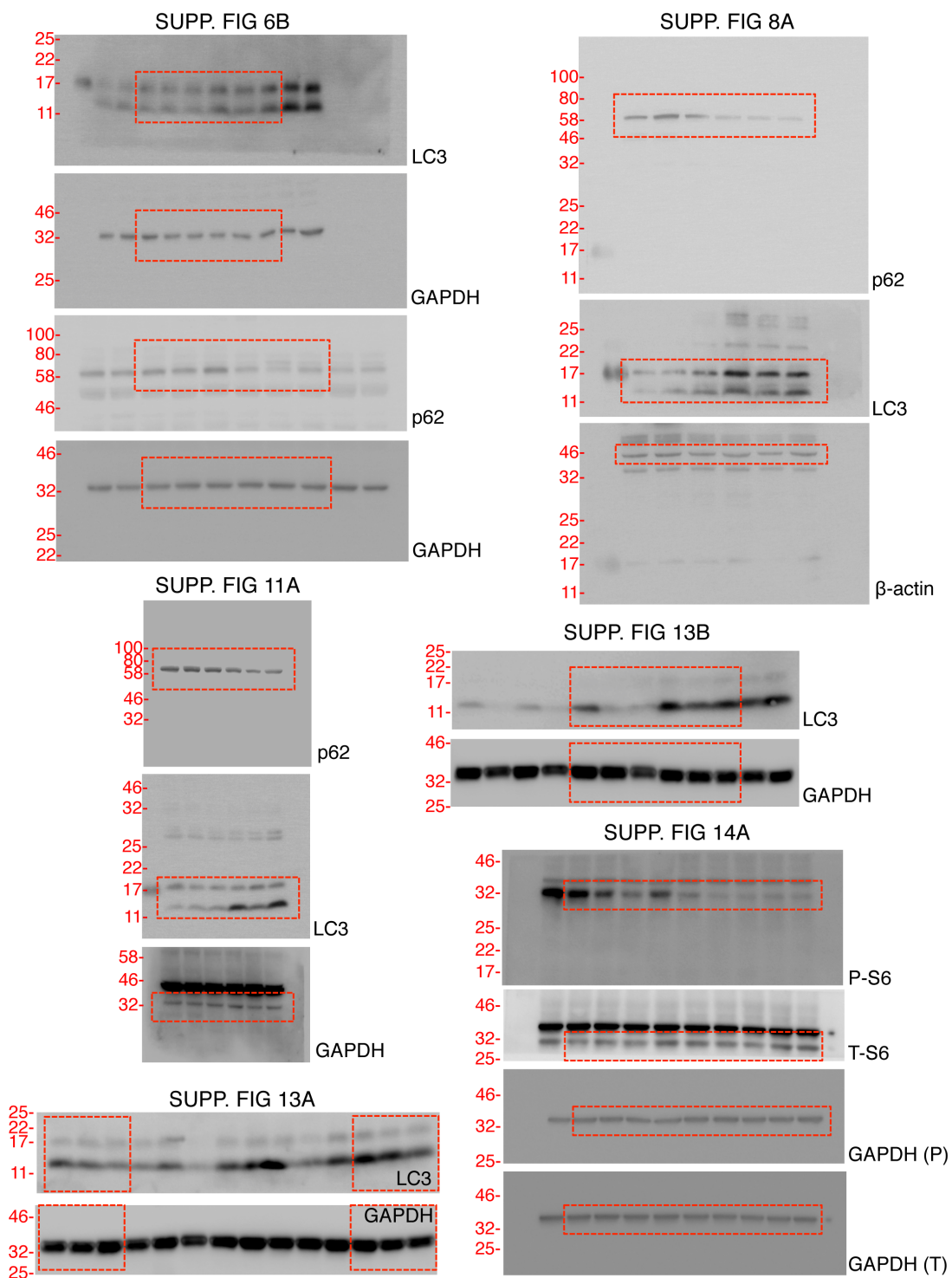


Fig. S15. Uncropped scans of western blots. Part 4.

SI appendix, SI Material and Methods

Detailed mouse procedures. To induce acute hyperammonemia (1), mice were overnight starved before the intraperitoneal (i.p.) injections of 10 mmol/kg of ammonium chloride (Merck) dissolved in water. Colchicine (Sigma-Aldrich; 0.4 mg/kg, for three days before the ammonia i.p. injections) (2) and Tat-Beclin-1 peptide (Millipore; 20 mg/kg, for two hours before the ammonia i.p. injections) (3), were dissolved in water and injected i.p. Rapamycin (Enzo Life Sciences; 2.0 mg/kg, for three days before the ammonia i.p. injections) (4) was re-suspended in 10% Dimethyl Sulfoxide (DMSO), 5% Tween-20 in saline solution and delivered by i.p. injection. Dimethyl- α -ketoglutarate (DMKG) (Sigma-Aldrich; 500 mg/kg, for three days and 1 hour prior to the ammonia i.p. injections) was dissolved in phosphate-buffered saline (PBS) solution and delivered by i.p. injections. Thioacetamide (Sigma-Aldrich) was re-suspended in saline solution and injected i.p. at the dose of 250 mg/kg (5). Three days prior to the administration of thioacetamide, mice were injected i.p. daily with Rapamycin or Tat-Beclin-1 peptide at the doses of 2.0 mg/kg and 15 mg/kg, respectively. To induce chronic hyperammonemia age-matched male mice were fed ad libitum with either a standard diet or a standard diet supplemented with 20% (w/w) of ammonium acetate (Mucedola s.r.l., Milan, Italy), as previously reported (6). Rapamycin was delivered by i.p. injections at 2.0 mg/kg every 48 hours for four consecutive weeks. Control mice were injected with vehicle only. HDAd-Cre, HDAd-TFEB, and HDAd-AFP were injected in volume of 200 μ l in the retro-orbital plexus. For mouse *Atg7* knock-down, *Atg7^{fl/fl}* mice were injected with a dose of 5×10^{12} vector particles (vp)/kg of HDAd-Cre or HDAd-AFP as a control. For the hepatic TFEB gene transfer, C57BL/6 wild-type mice were injected with a dose of 1×10^{13} vp/kg of HDAd-TFEB or HDAd-AFP as control. The ammonia i.p. challenge in these mice was performed at 4 weeks post-vector injection. Blood samples were collected by retro-orbital bleedings at the indicated time-points. Mice were sacrificed by cervical dislocation, and liver samples were harvested for analyses. The *spf^{ash}* mice were injected i.p. with 10 mg/kg of rapamycin (re-suspended in 10% DMSO, 5% Tween-20 in saline solution) or vehicle (10% DMSO, 5% Tween-20 in saline solution) daily for seven days. At the end of the experiment mice were euthanized in a carbon dioxide chamber and liver samples were harvested for analyses. Ureagenesis assay was performed as reported previously (7)

and blood samples were collected before the injection of the tracer, and at 30 min after the injection of the tracer. Assays were carried out before the injection of rapamycin or vehicle (basal samples) and on days 3 and 7 post-injection.

Dried blood spots (DBS, filter cards IDBS-226, Perkin Elmer, USA) were collected just before the ureagenesis assay to quantify orotic acid according to a published method (7) with some modification. Internal standard extraction solution was prepared as recommended in the Chromsystems kit insert with the addition of 10 μ M labeled orotic acid. One DBS punch (3 mm diameter) was placed in a microtiter plate and after addition of 100 μ L internal standard extraction solution, the microtiter plate was sealed with a plastic cover and incubated for 45 min at 45°C with shaking (750 rpm). After incubation, the organic extract was measured on a UPLC-MS/MS (Waters Xevo TQD, Milford, USA) with direct flow injection. Orotic acid was quantified against the labeled orotic acid in negative ion mode. MS/MS settings and transitions were as follows: for orotic acid/labeled orotic acid, dwell time 0.5 s, cone voltage 24.0 V, collision energy 10.0 eV, parent ion 154.94/156.94 Da, and daughter ion 110.93/112.93 Da. OTC enzyme analysis in liver extract was performed as described previously (8).

HDAd vectors. HDAd-Cre, HDAd-TFEB, and HDAd-AFP vectors all bear a liver-specific expression cassette (9) driving the expression of Cre recombinase, human TFEB or baboon AFP, respectively. HDAd vectors were produced as previously reported (9). 116 cells were regularly tested and found to be negative for *Mycoplasma* by quantitative real time PCR.

Analyses of serum and liver samples. Serum and liver ammonia content were measured by an ammonia colorimetric assay (BioVision Incorporated; Cat# K370-100) according to the manufacturer's instructions. Serum and liver urea content was determined in liver homogenates by an assay kit based on the Jung's method (BioVision Incorporated; Cat# K376-100). Serum and liver glutamine content was measured by a colorimetric assay kit (BioVision Incorporated; Cat# K556-100). Quantitation of hepatic acetyl-coA (BioVision Incorporated; Cat# K317-100) was performed by a fluorometric assay kit. Liver Cathepsin B activity was measured by a fluorometric assay kit (BioVision Incorporated; Cat# K140-100). Serum alanine aminotransferase (ALT) was measured by a colorimetric

assay kit (EnzyChrom™; Cat# EALT-100). Liver content of aspartate and glutamate was measured by high-performance liquid chromatography (HPLC) at the Biochemical Genetics Laboratories at Baylor College of Medicine (Houston, TX, USA). Hepatic alpha-ketoglutarate was determined by a fluorometric assay kit (BioVision Incorporated; Cat# K677-100). Liver lysates were made by homogenization in the corresponding hydrolysis buffer using a Tissue Lyser (Qiagen). All hepatic metabolite levels were normalized for protein concentrations determined by Bradford Reagent (Bio-Rad).

Preparations of total hepatic membrane (lysosomes) and cytosolic fractions. Liver samples were homogenized in four volumes of 0.3 M sucrose in the presence of complete phosphatase and protease inhibitor cocktail (Sigma). Liver lysates were subjected to low-speed centrifugation to obtain post-nuclear supernatants and then centrifuged at 100,000 g for 25 min, yielding total hepatocyte membranes containing the lysosomal fraction. The supernatant made by the organelle-free cytosolic fraction was collected. The pellet was washed four times (at 100,000 g for 25 min), and re-suspended in 0.3 M sucrose with phosphatase and protease inhibitors.

Preparations of nuclear hepatic fractions. Nuclear and cytoplasmic fractions from livers samples were prepared by using the CellLytic™ NuCLEAR™ Extraction Kit (Sigma, Cat# NXTRACT-1KT) according to the manufacturer's instructions.

Western blotting. Liver specimens were homogenized in RIPA buffer in the presence of complete phosphatase and protease inhibitor cocktail (Sigma), incubated for 20 min at 4°C and centrifuged at 13,200 rpm for 10 min. Pellets were discarded and cell lysates were used for western blots. Total protein concentration in cellular extracts was measured using the Bradford Reagent (Bio-Rad). Protein extracts, were separated by SDS-PAGE and transferred onto polyvinylidene difluoride (PVDF) membranes. Blots were blocked with TBS-Tween-20 containing 5% non-fat milk for 1 hr at room temperature, followed by incubation with primary antibody overnight at 4°C. The primary antibodies used were: rabbit anti-LC3B (Novus Biologicals; Cat# NB-100-2220), mouse anti-p62 (Abnova; Cat# H00008878-M01), mouse anti-NRB1 (Abnova; Cat# H00004077-M01), mouse anti-β-actin (Novus Biologicals; Cat# NB600-501), mouse anti-GAPDH (Santa Cruz Biotechnology; Cat# sc-32233), rabbit anti-phospho (P)-P70S6K (Cell Signaling

Technology; Cat# 9234), rabbit anti-P70S6K (Cell Signaling Technology; Cat# 9202), rabbit anti-P-S6 (Cell Signaling Technology; Cat# 2211), rabbit anti-S6 (Cell Signaling Technology; Cat# 2217), rabbit anti-P-AMPK (Cell Signaling Technology; Cat# 2535), rabbit anti-AMPK (Cell Signaling Technology; Cat# 5831), rabbit anti-mTOR (Cell Signaling Technology; Cat# 2983), rabbit anti-LAMP1 (Cell Signaling Technology; Cat# 3243), mouse anti-Tubulin (Novus Biologicals; Cat# NB100-78470), rabbit anti-ATG7 (Cell Signaling Technology; Cat# 2631), rabbit anti-P-ERK1/2 (Cell Signaling Technology; Cat# 4370), mouse anti-ERK1/2 (R&D Systems, Inc.; Cat# MAB1576), rabbit anti-P-AKT (Cell Signaling Technology; Cat# 4058), rabbit anti-AKT (Cell Signaling Technology; Cat# 4691), rabbit anti-P-ULK1 (Cell Signaling Technology; Cat# 6888), rabbit anti-TFEB (Bethyl laboratories, Inc; Cat# A303-673A), and mouse anti-Rad50 (Santa Cruz Biotechnology; Cat# sc74460). Proteins of interest were detected with horseradish peroxidase (HRP)-conjugated goat anti-mouse or anti-rabbit IgG antibody (GE Healthcare). Peroxidase substrate was provided by ECL Western Blotting Substrate kit (Pierce). Densitometric analyses of the Western blotting bands were performed using ImageJ Software.

Immunofluorescence. Liver specimens were fixed with buffered 4% paraformaldehyde (PFA) overnight at 4°C, then washed with PBS and embedded in optimal cutting temperature (OCT, Sakura) compound after dehydration in 30% sucrose. 5- μ m cryo-sections were blocked for 10 min in 4% PFA, permeabilized with 0.2% Triton-PBS, incubated for 30 min with 75 mM NH₄Cl in PBS, blocked for 30 min with 5% milk, 10% donkey serum in PBS (blocking buffer 1), and then blocked for 60 min with, 5% donkey serum, 3% bovine serum albumin (BSA), 20 mM MgCl₂, 0.3% Triton in PBS (blocking buffer 2). Rabbit anti-GFP antibody (Novus Biologicals; Cat# NB-600-308) was used at 1:800 dilution in blocking buffer 2 for an overnight incubation at 4°C. The AlexaFluor-488 anti-rabbit antibody made in donkey (Invitrogen; Cat# A21206) was used as secondary antibody (1:200 dilution, 45 min). Nuclei were counterstained with 4',6-diamidino-2-phenylindole (DAPI, Invitrogen). Stained liver sections were mounted in mowiol, cover-slipped and examined under a Zeiss LSM 710 confocal laser-scanning microscope.

Electron microscopy (EM). For EM analyses, liver specimens were fixed in 1% glutaraldehyde in 0.2 M HEPES buffer. Small blocks of liver tissues were then post-fixed in uranyl acetate and OsO₄. After dehydration through a graded series of ethanol solutions, tissue samples were cleared in propylene oxide, embedded in epoxy resin (Epon 812) and polymerized at 60°C for 72 h. From each sample, thin sections were cut with a Leica EM UC6 ultramicrotome and images acquired by FEI Tecnai –12 (FEI, Eindhoven, The Netherlands) EM equipped with Veletta CCD camera for digital image acquisition. Morphometric analyses were performed using iTEM software (Olympus SIS, Germany).

Real time PCR. Total RNA from livers was extracted in TRIzol reagent (Invitrogen) using RNeasy mini kit (Qiagen). RNA was retro-transcribed using High-Capacity cDNA Reverse Transcription Kit (Applied Biosystems). The qPCR reactions were set up using SYBR Green Master Mix and run in duplicate on a Light Cycler 480 system (Roche). Running program was as follows: preheating, 5 minutes at 95°C; 40 cycles of 15 seconds at 95°C, 15 seconds at 60°C, and 25 seconds at 72°C. The β_2 -microglobulin gene was used as endogenous control. Fold changes were calculated using the DDCT method. Lysosomal and autophagic gene-specific primers were previously reported (10-12). Primers for TFEB were designed to amplify both human and mouse TFEB, as previously (9). Urea cycle gene-specific primers were previously described (13).

Determination of ¹⁵N-labeled urea by nuclear magnetic resonance spectroscopy (NMR). C57BL/6 wild-type mice injected i.p. with Tat-Beclin-1 or vehicle prior to the i.p. injection of 10 mmol/kg of ¹⁵N-labeled ammonium chloride (98% enriched in ¹⁵N, Sigma). Blood samples were collected by retro-orbital bleedings at 0, 5, 10, 15, and 30 min post-injection. The amount of ¹⁵N-labeled urea in sera was evaluated by comparison to ¹⁵N-leucine signal added to all samples as an internal reference. Biological ¹⁵N-labeled urea in each sample was quantified from the observed ¹⁵N peak intensities (in integrated areas) compared to the internal standard. One-dimensional (1D) ¹⁵N spectra were recorded at 44.55 MHz on a Bruker AVANCE™III HD-400 spectrometer, equipped with a BBO BB-H&F-D CryoProbe™ Prodigy fitted with a gradient along the Z-axis, at a probe temperature of 27°C (300 K). The pulse Ineptd sequence (INEPT for non-selective polarization transfer with decoupling during acquisition) was used with the following

parameters: $d1 = 5$ s, $J = 9$ 0Hz, $ns = 15000$ and acquisition time of 0.809 s. The leucine signal was assumed to resonate at 18.00 ppm, and therefore the urea signal resonated at 55.80 ppm.

Metabolite profiling of liver tissue by $^1\text{H-NMR}$. Tissues were mechanically disrupted to extract the metabolites of interest (lipids, carbohydrates, amino acids, and other small metabolites) while leaving others compounds (DNA, RNA, and proteins) in the tissue pellet. Homogenization of 200 mg of frozen tissue samples was carried out in 8 ml/g of wet tissue made of methanol and 1.70 ml/g per wet tissue of water (all solvents were cold) with UltraTurrax for 2 min on ice. Four ml/g wet tissue of chloroform were added and the homogenate was gently stirred and mixed on ice for 10 min (the solution must be mono-phasic). Then, additional 4 ml/g wet tissue of chloroform and 4 ml/g wet tissue of water were added and the final mixture was well shaken and centrifuged at 12,000 g for 15 min at 4°C. This procedure separates three phases: water/methanol on the top (aqueous phase with the polar metabolites), denatured proteins and cellular debris in the middle, and chloroform at the bottom (lipid phase with lipophilic compounds). The upper and the lower layers were transferred into glass vials, the solvents removed under a stream of dry nitrogen, and stored at -80°C until the analyses.

$^1\text{H-NMR}$ measurements of polar metabolites. The polar extracts were re-suspended in 700 μl PBS, pH 7.4 with 10% D_2O for lock procedure, and then transferred into an NMR tube. One-dimensional (1D) spectra were recorded at 600.13 MHz on a Bruker Avance III-600 spectrometer equipped with a TCI CryoProbeTM fitted with a gradient along the Z-axis, at a probe temperature of 27°C, using the excitation sculpting sequence for solvent suppression. Spectra were referred to internal 0.1 mM sodium trimethylsilylpropionate (TSP), assumed to resonate at $\delta = 0.00$ ppm.

NMR data processing and statistical analysis. The spectral 0.50–9.40 ppm region of the high-resolution $^1\text{H-NMR}$ spectra was automatically data reduced to integrated regions (buckets) of 0.04-ppm each using the AMIX 3.6 package (Bruker Biospin, Germany). The residual water resonance region (4.72–5.10 ppm) was excluded, and the integrated region was normalized to the total spectrum area. To differentiate liver tissues through NMR spectra, we carried out a multivariate statistical data analysis using projection

methods. The integrated data reduced format of the spectra was imported into SIMCA-P+ 15 package (Umetrics, Umea, Sweden), and PCA and O2PLS discriminant analyses (O2PLS-DA) were performed. Meancentering was applied as data pre-treatment for PCA, while Pareto scaling and mean centering were used prior to O2PLS-DA. PCA is a well-known unsupervised technique designed to extract and display the systematic variation in a data matrix in order to identify trends and clusters. O2PLS is a multivariate regression method that extracts linear relationships from two data blocks, X and Y, by removing the structured noise. In particular, O2PLS decomposes the systematic variation in the X-block into two model parts: the so-called predictive part, which models the correlations between X and Y and another called the orthogonal part, which is not related to Y. Like other PLS regression techniques, O2PLS can be used to perform discriminant analysis by introducing suitable dummy variables. The main advantage in using O2PLS-DA technique is the reduction of the model complexity. For N classes, the dimension of the predictive space is N-1, and the classification model can be investigated by using only N-1 latent components. The p(corr)/q(corr) or S-plots were used to highlight the role of the X-variables in the classification model.

Pathway Analysis. Metabolite Set Enrichment Analysis (MSEA) to identify biologically meaningful patterns that are significantly enriched in selected and more representative metabolites in class separation was applied to the pathway topology search tool in Metaboanalyst 3.0 (14, 15). In this analysis, metabolic “pathway-associated metabolite sets” (currently containing 88 entries) from human library were selected. Over Representation Analysis was implemented using the hypergeometric test to evaluate whether a particular metabolite set is represented more than expected by chance within the selected compound list. Metabolites were selected by evaluating both VIP values > 1 in class discrimination and correlation values $|p(\text{corr})| > 0.7$.

References

1. Ye X, et al. (1997) Adenovirus-mediated in vivo gene transfer rapidly protects ornithine transcarbamylase-deficient mice from an ammonium challenge. *Pediatr Res* 41(4 Pt 1):527-534.

2. Shoji-Kawata S, et al. (2013) Identification of a candidate therapeutic autophagy-inducing peptide. *Nature* 494(7436):201-206.
3. Ju JS, Varadhachary AS, Miller SE, & Wehl CC (2010) Quantitation of "autophagic flux" in mature skeletal muscle. *Autophagy* 6(7):929-935.
4. Ni HM, et al. (2012) Activation of autophagy protects against acetaminophen-induced hepatotoxicity. *Hepatology* 55(1): 222-232.
5. Nicaise C, et al. (2008) Control of acute, chronic, and constitutive hyperammonemia by wild-type and genetically engineered *Lactobacillus plantarum* in rodents. *Hepatology* 48(4):1184-1192.
6. Azorin I, Minana MD, Felipo V, & Grisolia S (1989) A simple animal model of hyperammonemia. *Hepatology* 10(3):311-314.
7. Allegri G, et al. (2017) A simple dried blood spot-method for in vivo measurement of ureagenesis by gas chromatography-mass spectrometry using stable isotopes. *Clin Chim Acta* 464:236-243.
8. Rivera-Barahona A, et al. (2015) Functional characterization of the spf/ash splicing variation in OTC deficiency of mice and man. *PloS one* 10(4):e0122966.
9. Pastore N, et al. (2013) Gene transfer of master autophagy regulator TFEB results in clearance of toxic protein and correction of hepatic disease in alpha-1-antitrypsin deficiency. *EMBO Mol Med* 5(3):397-412.
10. Qiu J, et al. (2012) Hyperammonemia-mediated autophagy in skeletal muscle contributes to sarcopenia of cirrhosis. *Am J Physiol Endocrinol Metab* 303(8):E983-993.
11. Settembre C, et al. (2011) TFEB links autophagy to lysosomal biogenesis. *Science* 332(6036):1429-1433.
12. Settembre C, et al. (2012) A lysosome-to-nucleus signalling mechanism senses and regulates the lysosome via mTOR and TFEB. *EMBO J* 31(5):1095-1108.
13. Piccolo P, et al. (2017) Down-regulation of hepatocyte nuclear factor-4 alpha and defective zonation in livers expressing mutant Z alpha1-antitrypsin. *Hepatology* 66(1): 124-135.
14. Xia J, Wishart DS (2016) Using MetaboAnalyst 3.0 for Comprehensive Metabolomics Data Analysis. *Current Protocols in Bioinformatics*, 55:14.10.1-14.10.91.

15. Xia J, Wishart DS (2010) MSEA: a web-based tool to identify biologically meaningful patterns in quantitative metabolomic data. *Nucleic Acids Res* 38:W71-77.